National Physical Laboratory

AAPM 2022
JULY 10–14 | WASHINGTON, DC
64TH ANNUAL MEETING & EXHIBITION
CELEBRATING MEDICAL PHYSICS
TRANSFORMING HUMAN HEALTH

Challenges in FLASH beam dosimetry: Appropriate detectors to use

Anna Subiel, PhD, CPhys

Medical Radiation Science, National Physical Laboratory,
Hampton Road, Teddington, Middlesex, TW11 0LW, UK

The EMPIR initiative is co-funded by the European Union's Horizon 2020 research and innovation programme and the EMPIR Participating States

Outline

- Accuracy in RT
- Dosimetry for UHDR beams
  - Passive detectors
  - Active detectors
    - Ionization chambers
    - Diamond detectors
    - Calorimeters
- Summary and Conclusions

Requirement on Accuracy in RT

- The ICRU Rep.24 (1976) states:

An uncertainty of 5% is tolerable in the delivery of absorbed dose to the target volume

- This is interpreted to represent a confidence level of 1.5-2 times the SD
- Currently, the recommended accuracy of dose delivery is generally **5-7% (k=2)**

Given the size of the error in the biological contribution, it is important that the physical errors are minimized

Dosimetry for UHDR beams

NPL National Physical Laboratory

Passive dosimeters

- Alanine
- Radiochromic films
- TLDs
- Methyl viologen

dose rate independent

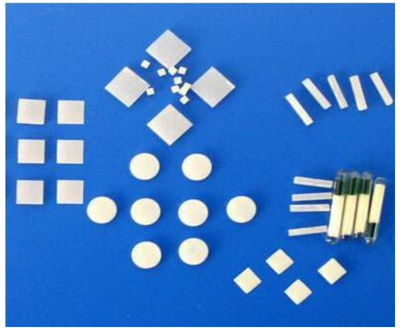

Dosimetry for UHDR beams

NPL National Physical Laboratory

Passive dosimeters

- Alanine
- Radiochromic films
- TLDs
- Methyl viologen

dose rate independent

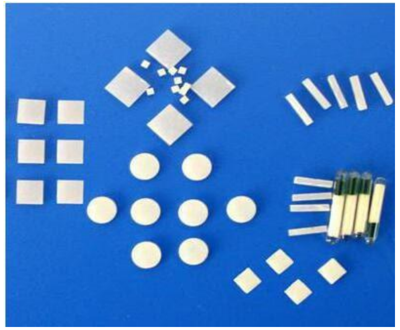

- linear relationship with the dose rate – dose rate independence
- water equivalence
- can be used for small fields measurements (TLDs, films, alanine)

- Complex and time-consuming evaluation process and post-irradiation processing
- Require calibration for each batch, which can be time consuming
- Large uncertainties **IF** the evaluation process not well established

Dosimetry for UHDR beams

Passive dosimeters

- Alanine
- Radiochromic films
- TLDs
- Methyl viologen

dose rate independent

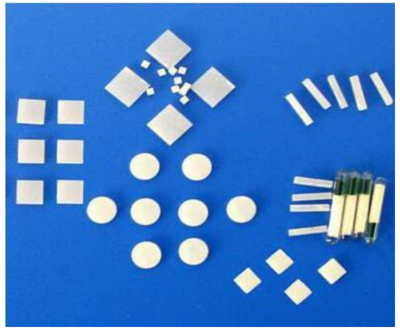

Example of proposed solution to reduce processing time

•Fast alanine dosimetry for FLASH RT by optimization of reading parameters
•The total reading time for the three measurements was 7.8 min with ±2% (k=1) uncert. (for doses above 10 Gy)
•To measure dose below 5Gy with uncert. below 5% (k=1) the reading time increased to 13 min

Gondré Rad.Res. 194:6 (2020)

Dosimetry for UHDR beams

Passive dosimeters

- Alanine
- Radiochromic films
- TLDs
- Methyl viologen

dose rate independent

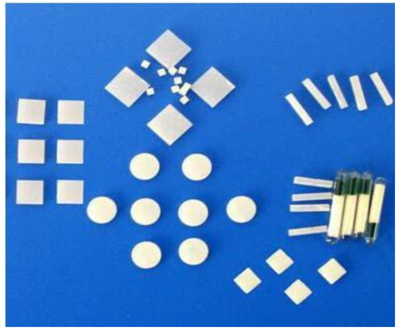

Active (online) **detectors**

- Ionization chambers
- Diamond detectors
- Calorimeters

dependence as a function of DPP

Ionization chambers

Ionization chamber

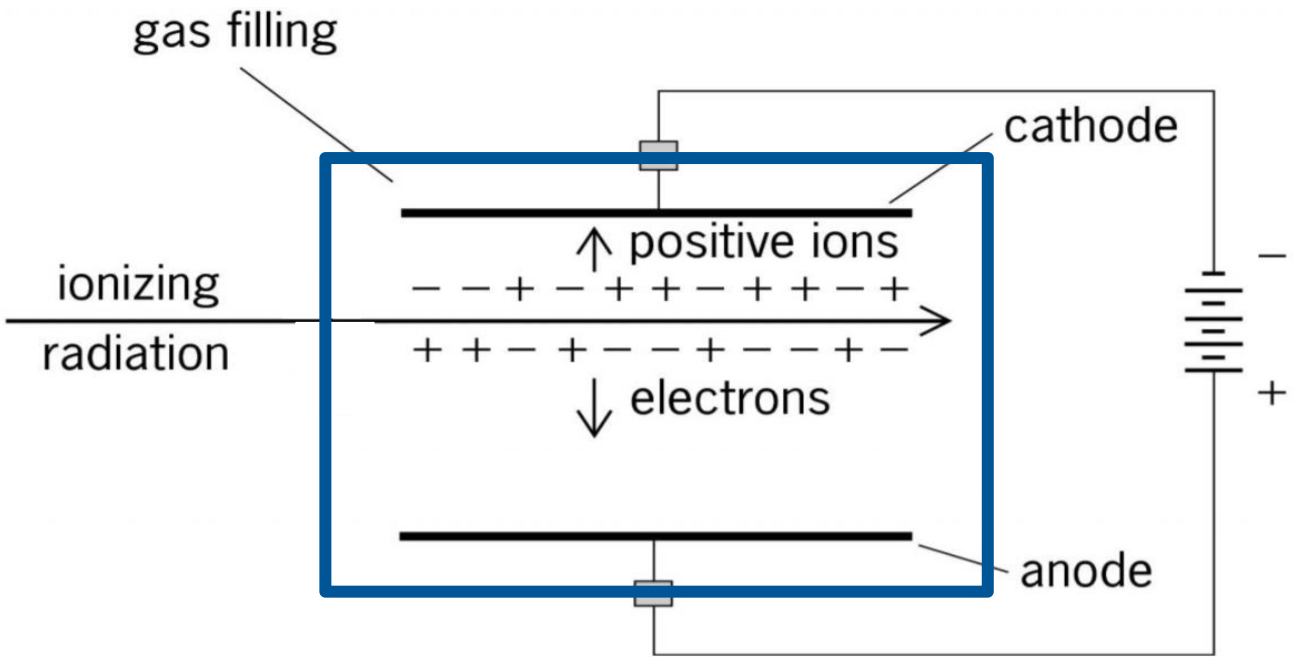

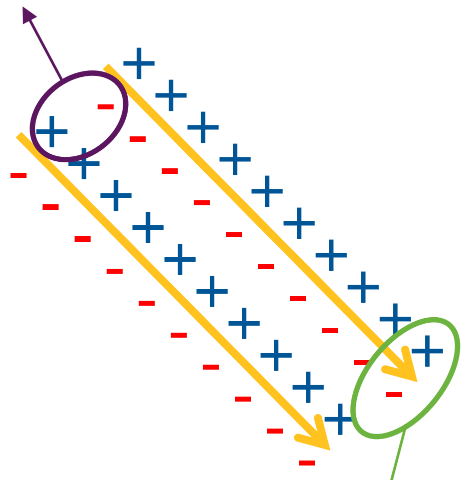

Initial Recombination

- Recombination along a single charged particle track.
- **Independent of dose and dose-rate**.
- More pronounced in highly ionising particles such as alpha-particles.

General Recombination

- Recombination between separate charged particle tracks.
- Directly dependent on charge density i.e the number of ions produced per unit volume.
- **Dose-rate dependent.**

General recombination is likely to play a much larger role in recombination effect in UHDR pulsed beams

Di Martino, et al. Med Phys. 32(7) (2005)

IC: Metrological challenges of dosimetry at UHDR

Typical behaviour of IC at FLASH dose rates

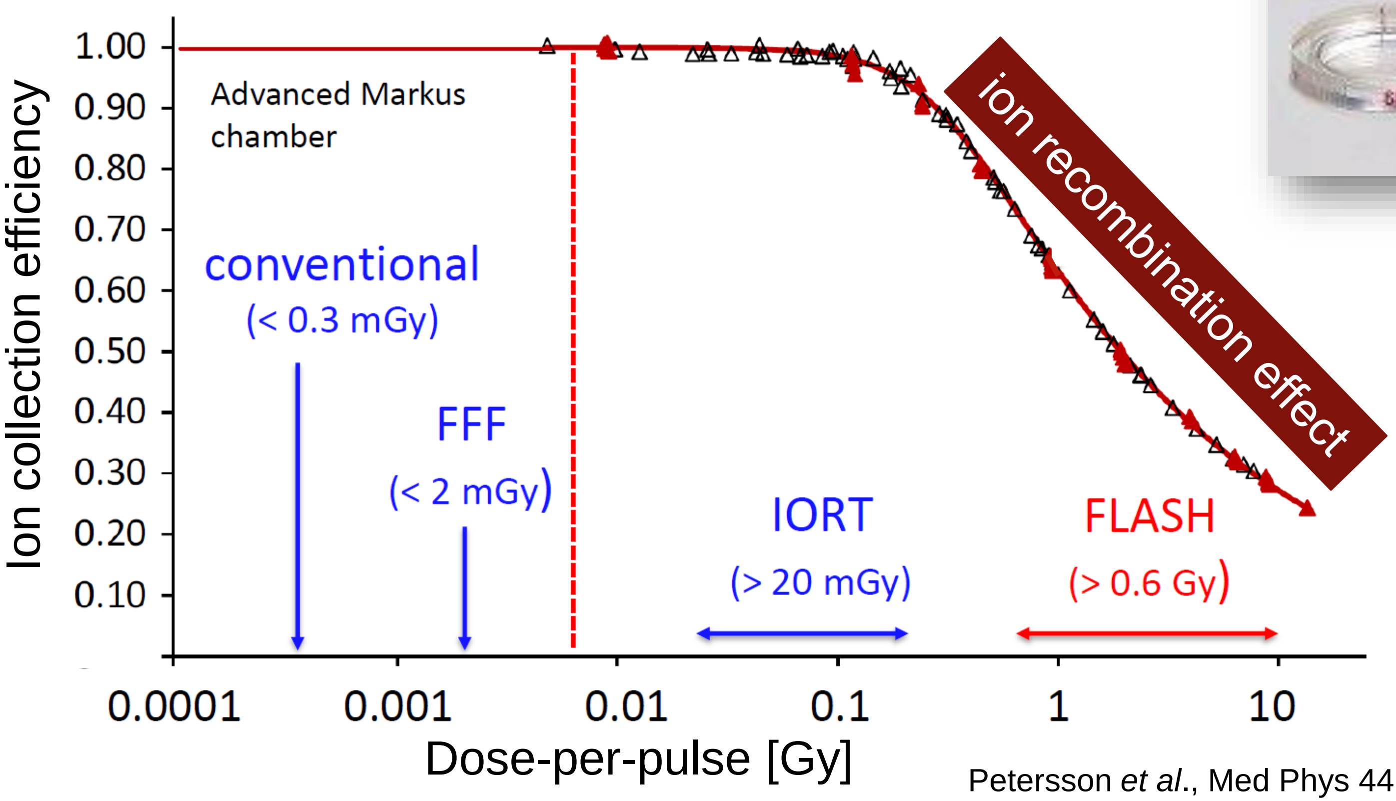

Petersson *et al.*, Med Phys 44 (2017) 1157

PTW Advanced Markus
(1 mm electrode separation)

$$k_s = \left(1 + \left(\frac{DPP[mGy]}{U[V]}\right)^{\alpha}\right)^{\beta}$$

no physical meaning

So far:

- Lack of primary standard for FLASH RT
- Lack of formalism for reference dosimetry
- Lack of active dosimeters for real-time measurements

IC: Metrological challenges of dosimetry at UHDR

NPL National Physical Laboratory

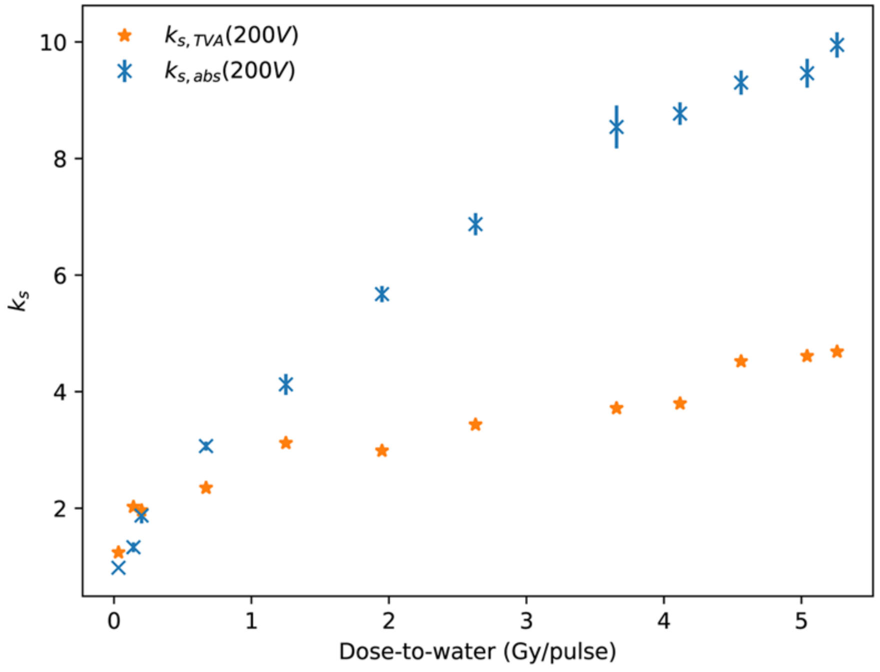

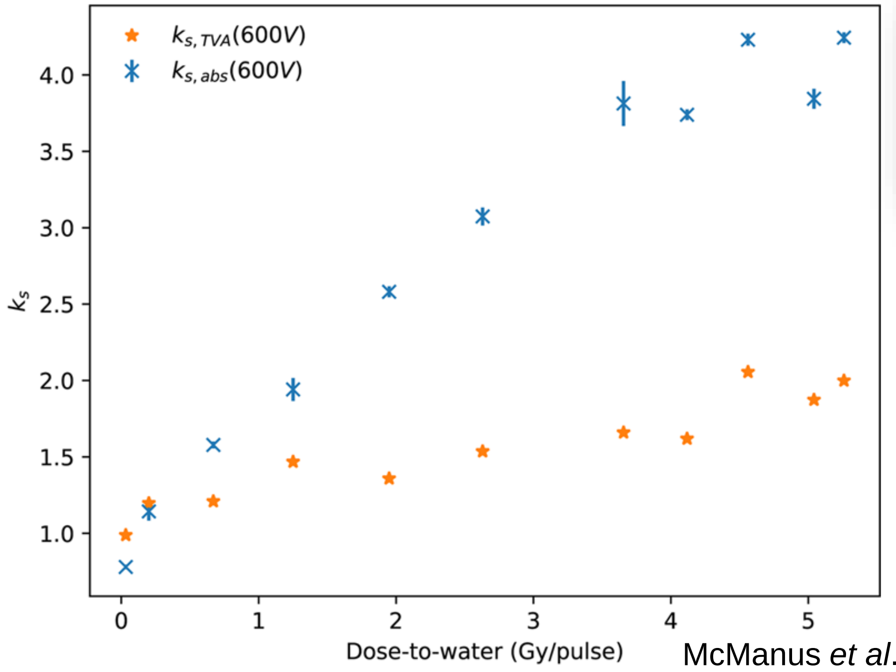

PTW Roos (2 mm electrode separation)

- 200 MeV VHEE beam
- DPP: 0.03 – 5.3 Gy/pulse
- Graphite calorimeter employed as reference detector

$$k_{s,abs} = \frac{D_{w,cal}}{M k_{pol} k_{TP} k_{Q,Q_0} N_{D,w,Q_0}}$$

McManus *et al.*, Sci. Rep. (2020)

- k_s up to 10 (V = 200 V) → **collection eff. 10%**
- k_s up to 4 (V = 600 V) → **collection eff. 25%**
- $k_{s,abs}$ compared with $k_{s,TVA}$ (two-voltage method)
- Available **analytical ion recombination models cannot predict chamber behaviour** for such a high DPP

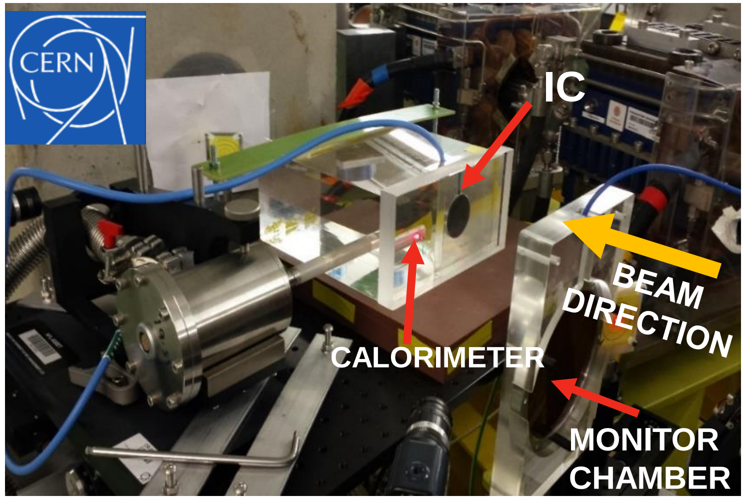

Possible solution for UHDR beams

USC's prototype ionization chambers for ultra-high DPP

Simulated ion recombination correction factor k_s for plane parallel ionization chambers at 300 V for **5 Gy/pulse**

Fig. Ionization chamber prototype (0.27 mm)

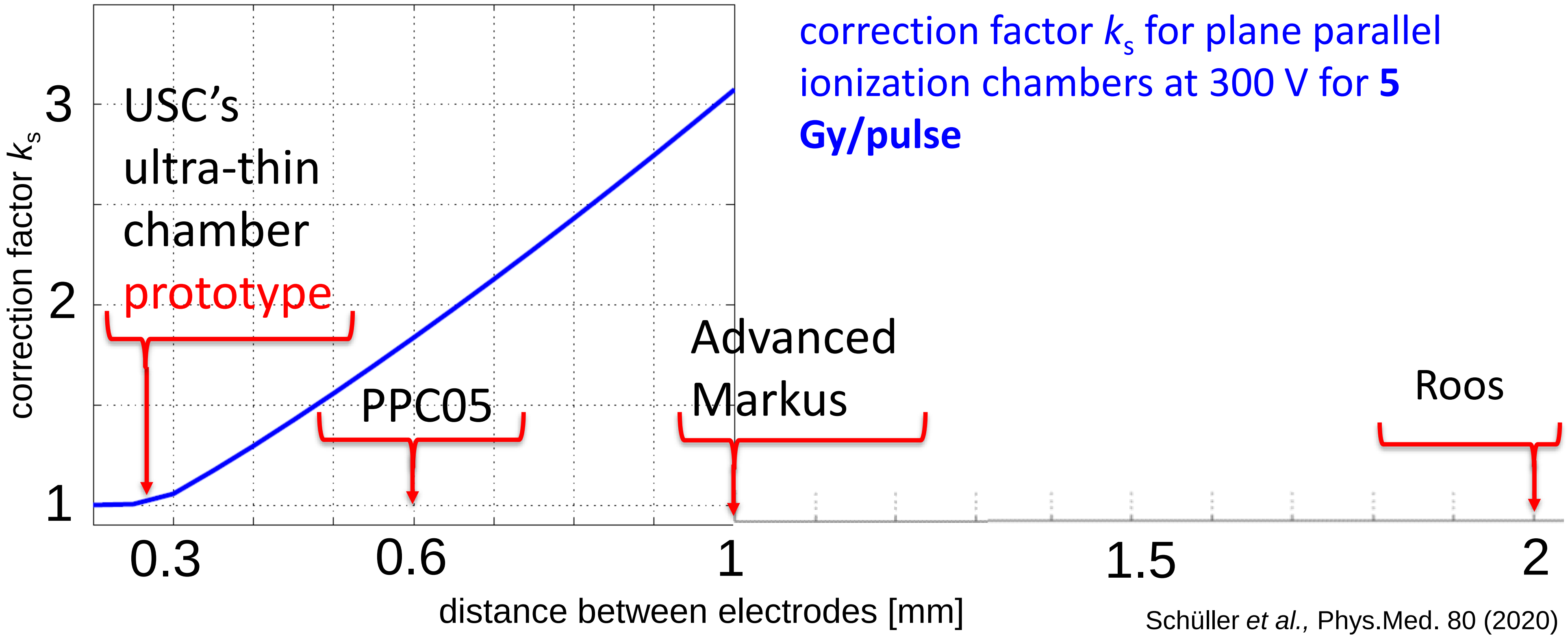

Schüller *et al.*, Phys.Med. 80 (2020)

Courtesy of Faustino Gomez

Possible solution for UHDR beams

USC's prototype ionization chambers for ultra-high DPP

Fig. Ionization chamber prototype (0.27 mm)

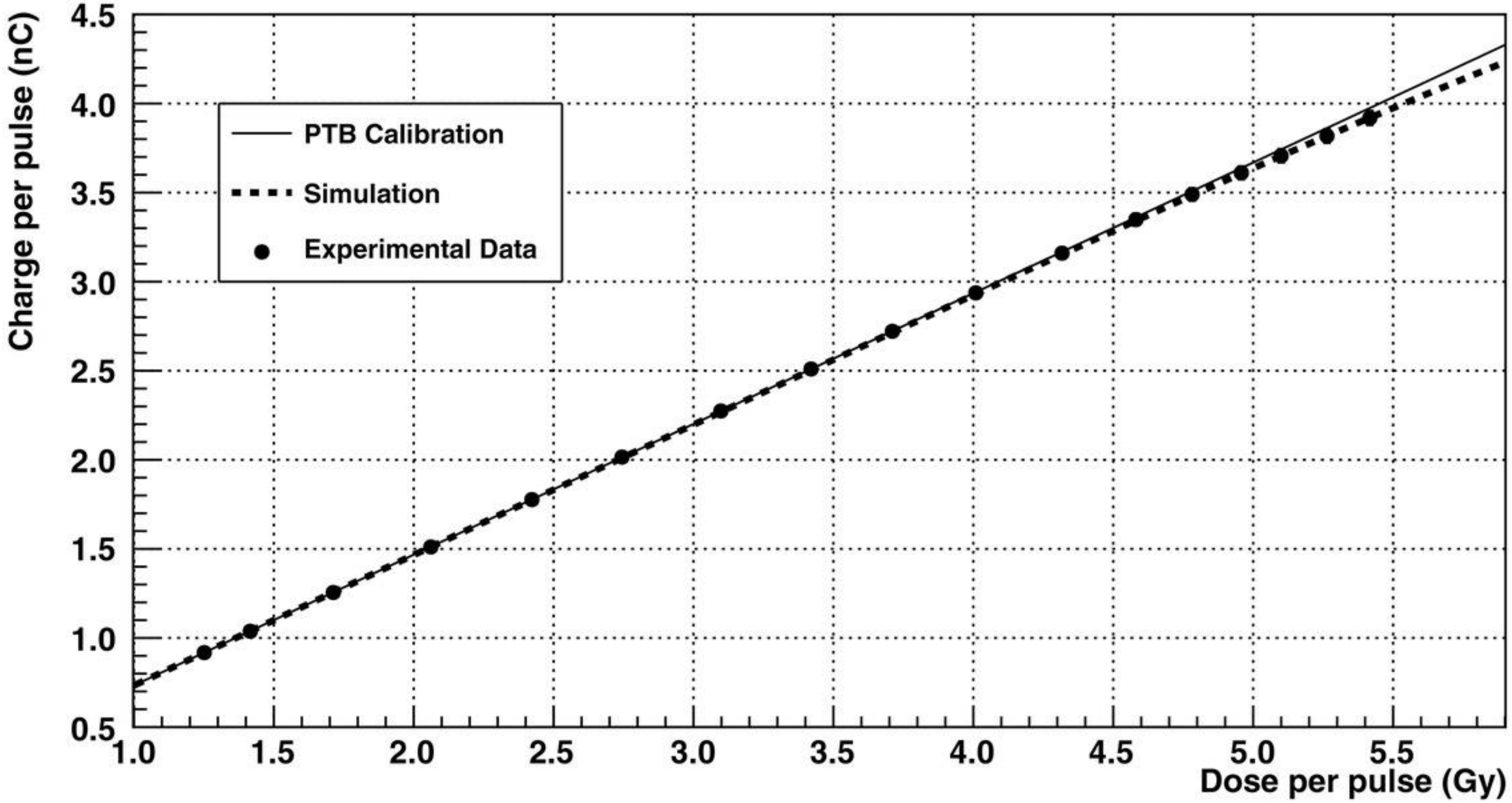

Courtesy of Faustino Gomez

Gomez *et al.*, Med.Phys.1-10 (2022)

Possible solution for UHDR beams

PTW's prototype ionization chambers for ultra-high DPP

Fig. PTW IC prototype (0.25 mm)

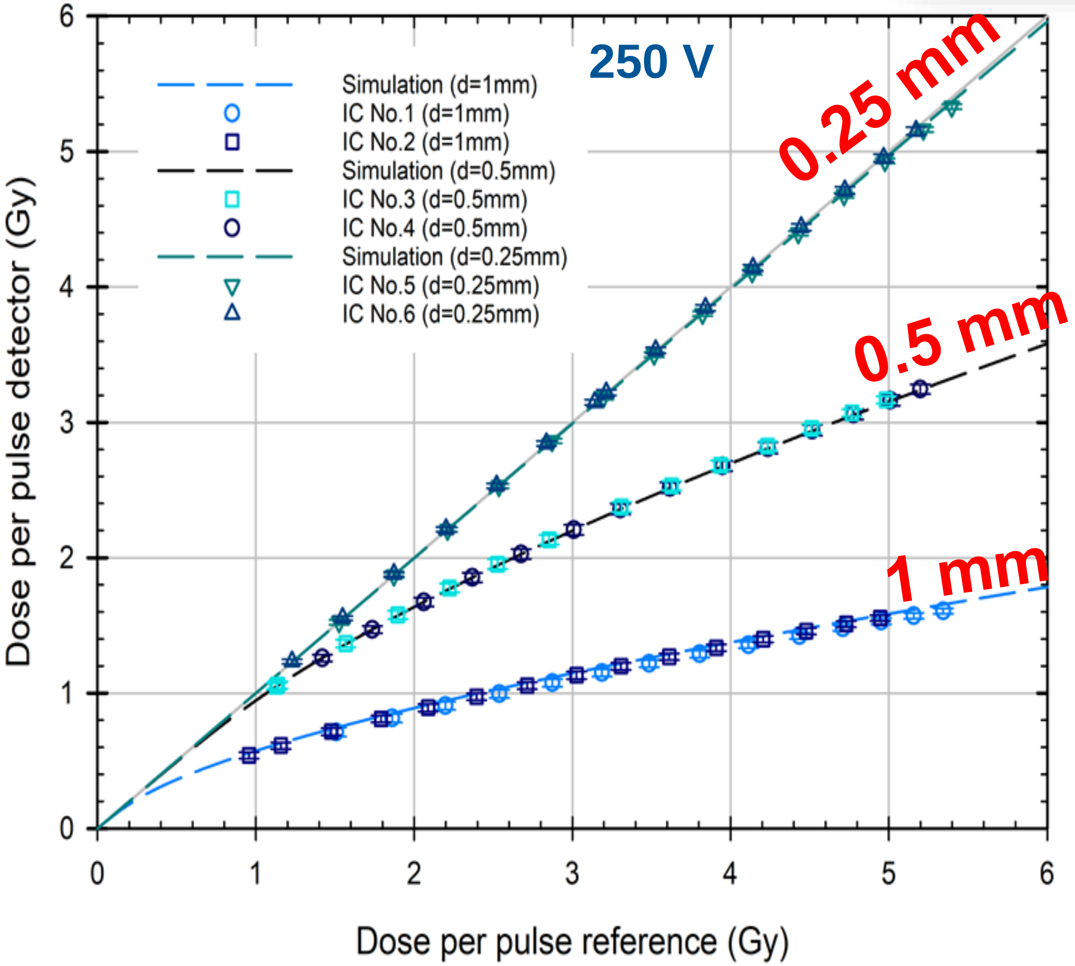

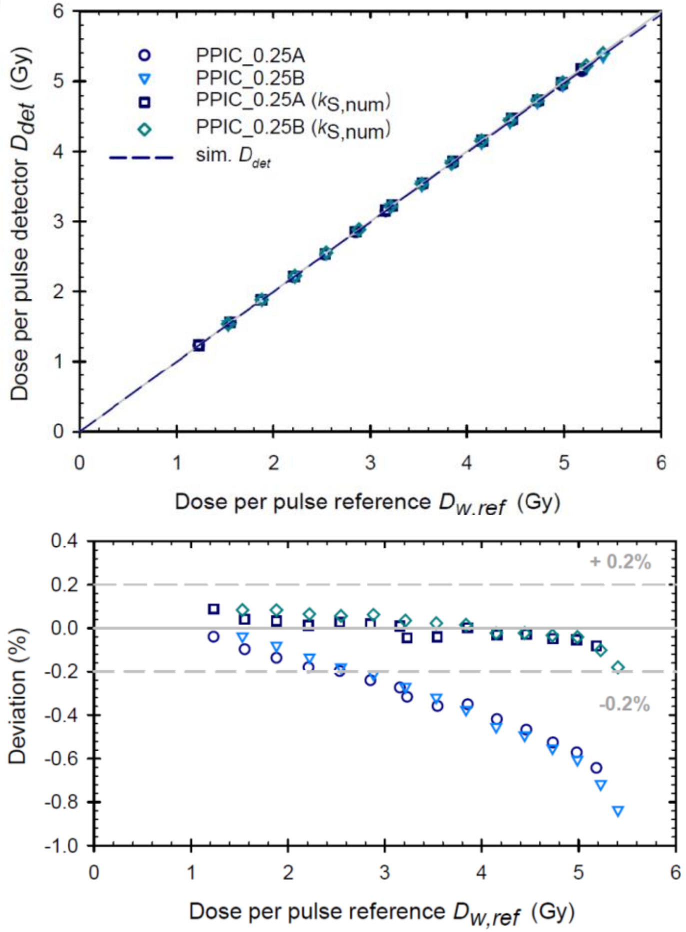

Courtesy of R. Kranzer

Kranzer *et al.*, Phys. Medica under review

Possible solution for UHDR beams

PTW's prototype ionization chambers for ultra-high DPP

Fig. PTW IC prototype (0.25 mm)

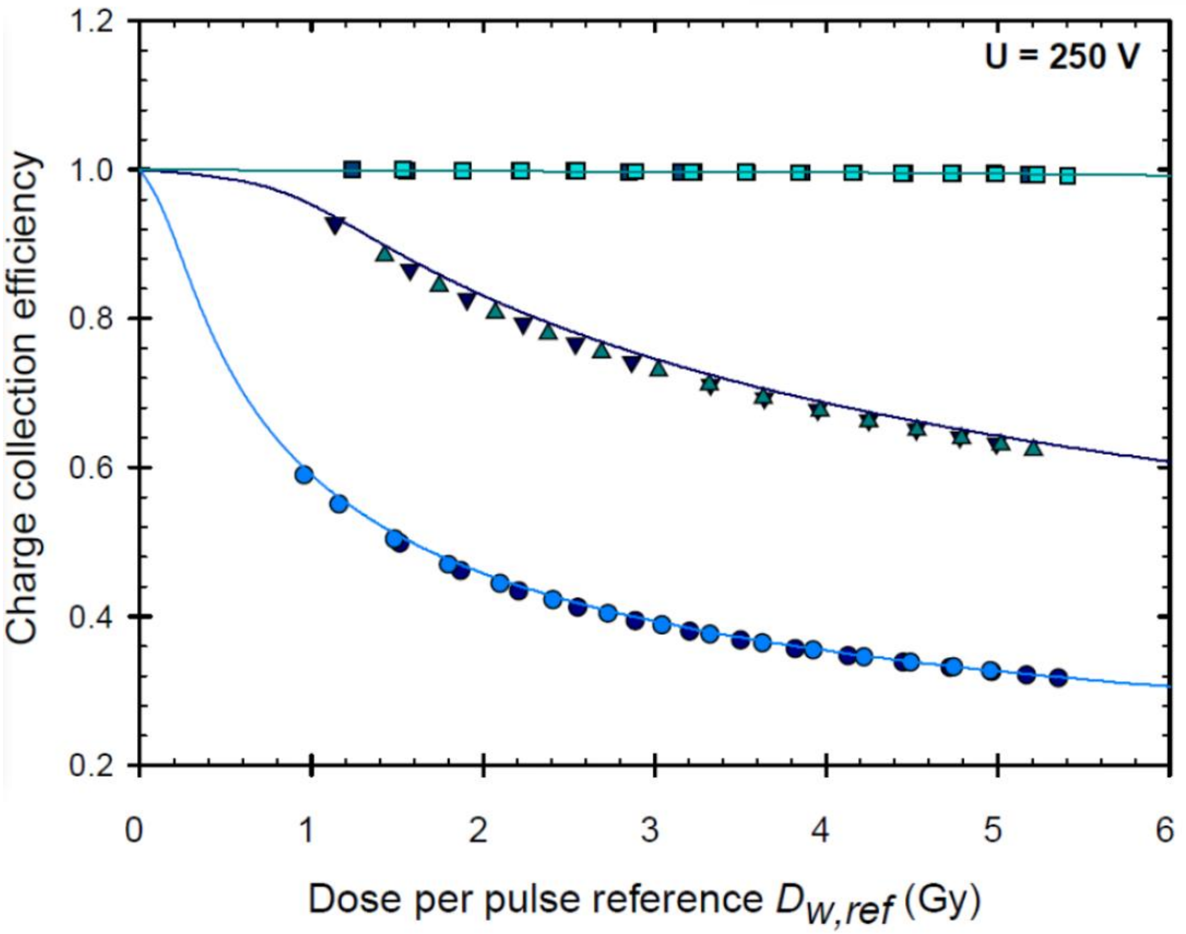

Courtesy of R. Kranzer

Kranzer *et al.*, Phys. Medica under review

National Physical Laboratory

Diamond detectors

Diamond detectors

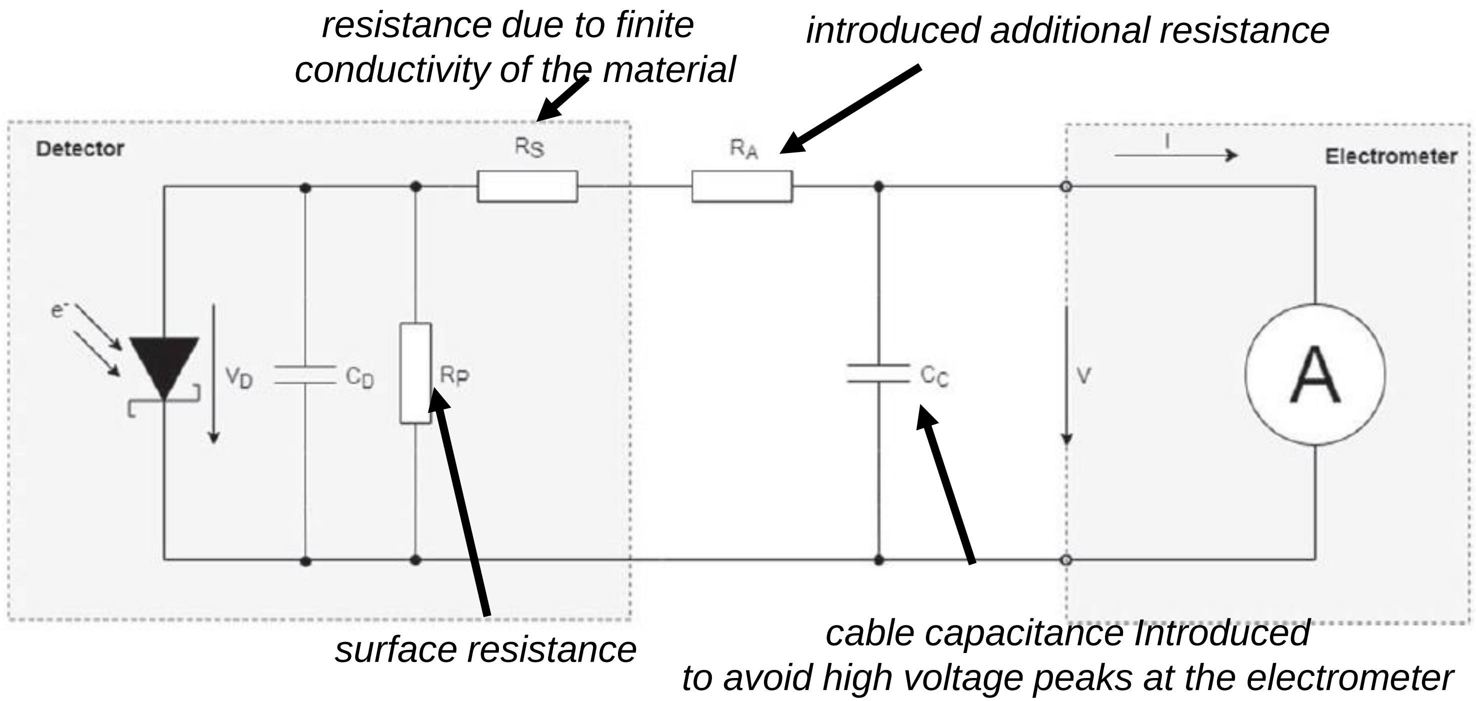

Fig. Circuit representing microDiamond detector (equivalent to diode)

- microDiamond detector operates as a Schottky diode

ADVANTAGES

- No ion recombination effects
- high water equivalence of the sensitive volume (in terms of effective atomic number)
- In contrast to air-filled ionization chambers, no conversion of ion dose to absorbed dose-to-water is necessary for PDD measurements.
- good stability of the response with regard to the accumulated dose
- high spatial resolution

Possible solution for UHDR beams

PTW's microDiamond for ultra-high DPP

Fig. microDiamond

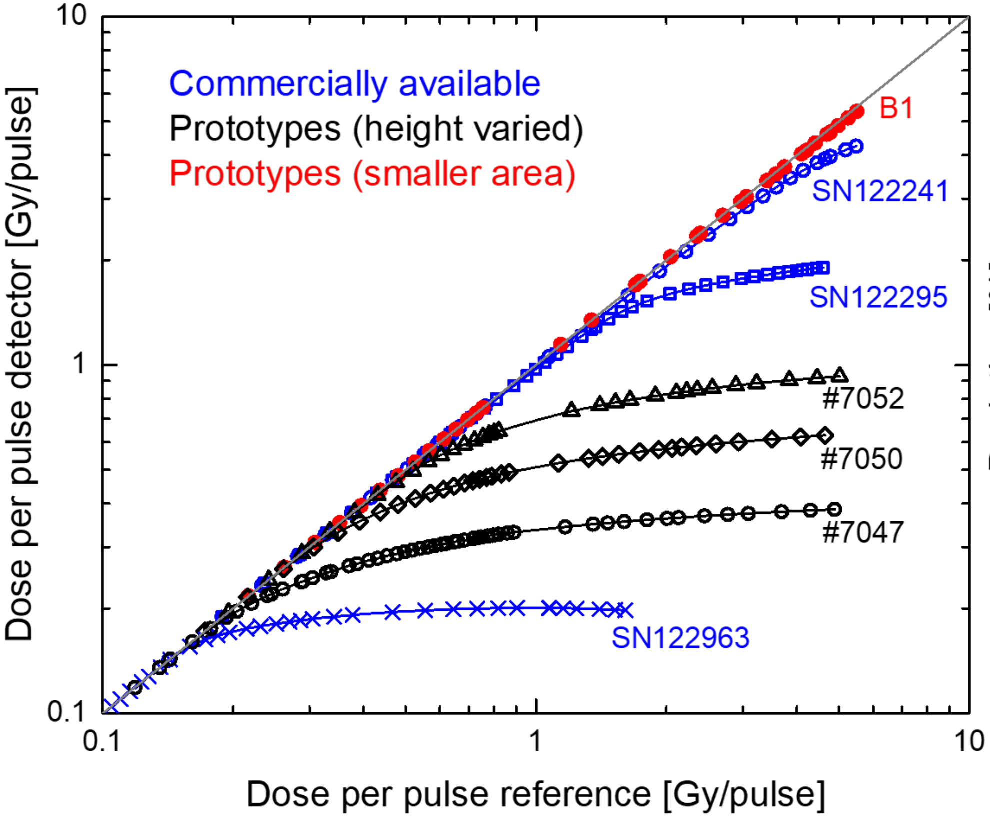

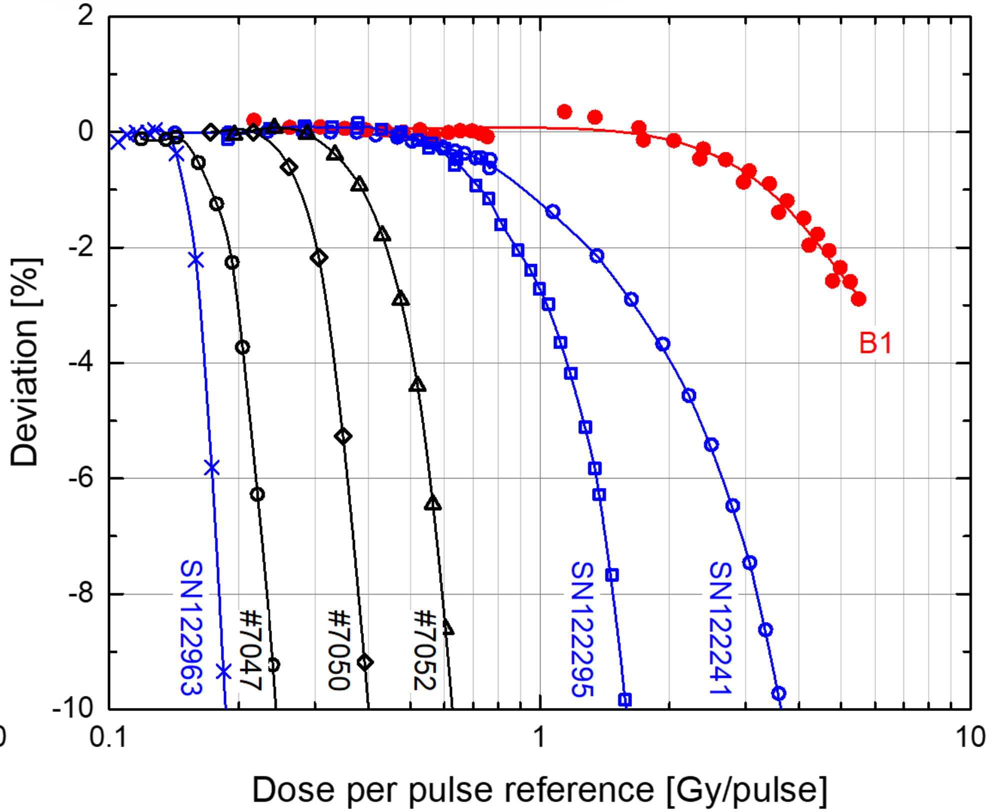

Courtesy of R. Kranzer

Kranzer *et al.*, *PMB 67 (2022)*

Possible solution for UHDR beams

PTW's microDiamond for ultra-high DPP

Fig. microDiamond

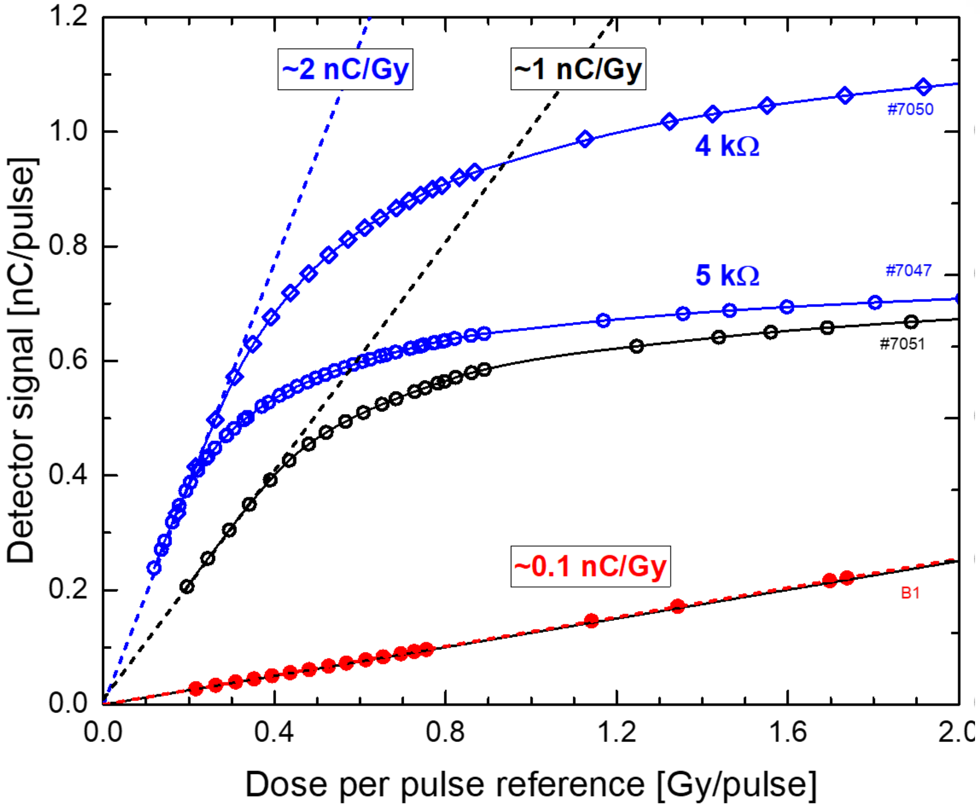

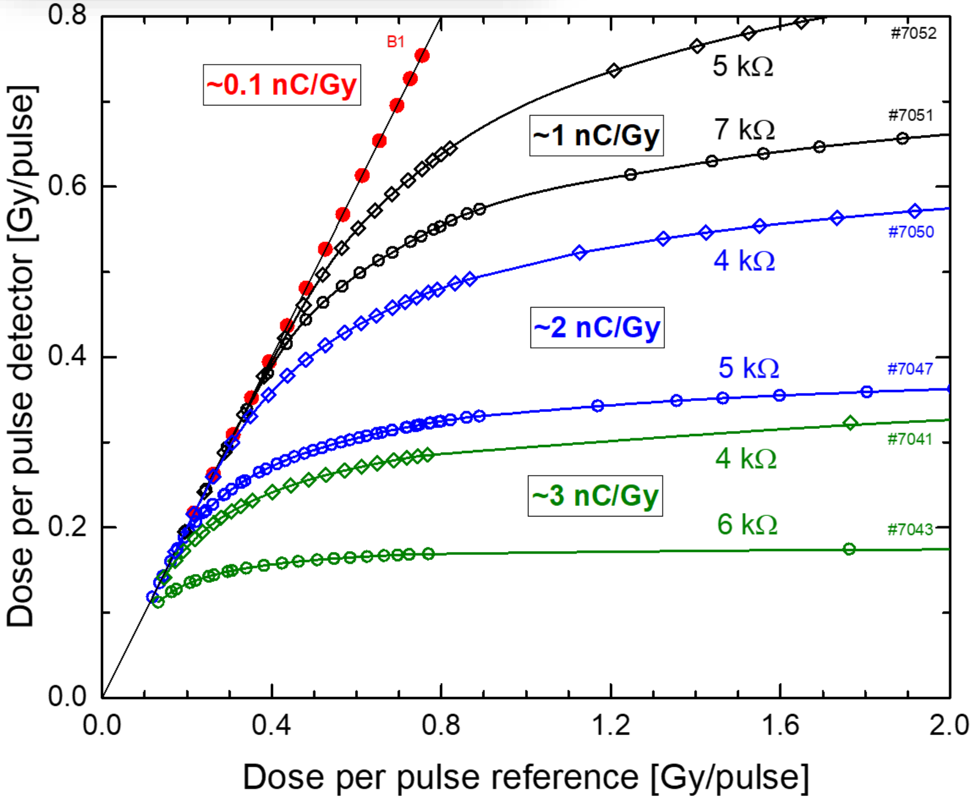

- Commercially available microDiamond detectors show saturation effects at different DPP levels.
- The linear range can be extended to the ultra-high DPP range by reduction of sensitivity and resistance.

Kranzer *et al.*, *PMB 67 (2022)*

Possible solution for UHDR beams

flashDiamond (fD) for ultra-high DPP

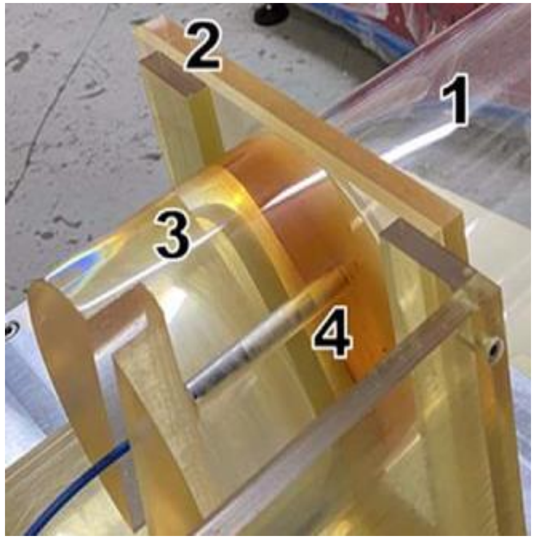

Fig. fD (4) positioned in the experimental setup

Marinelli *et al. Med. Phys*. **49** (2022)

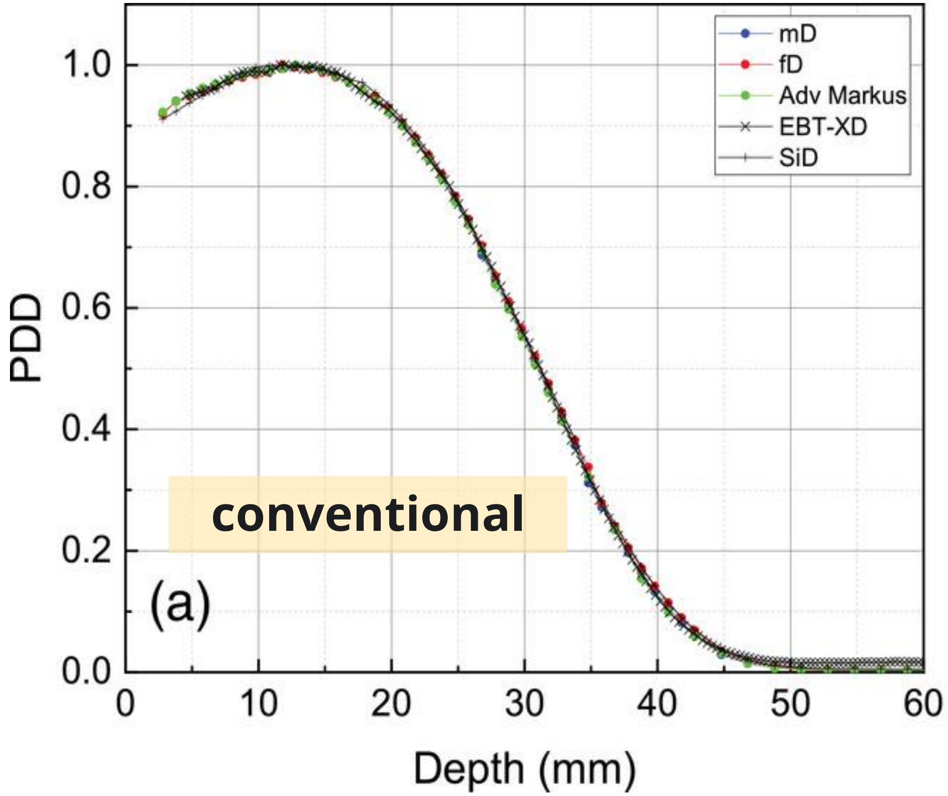

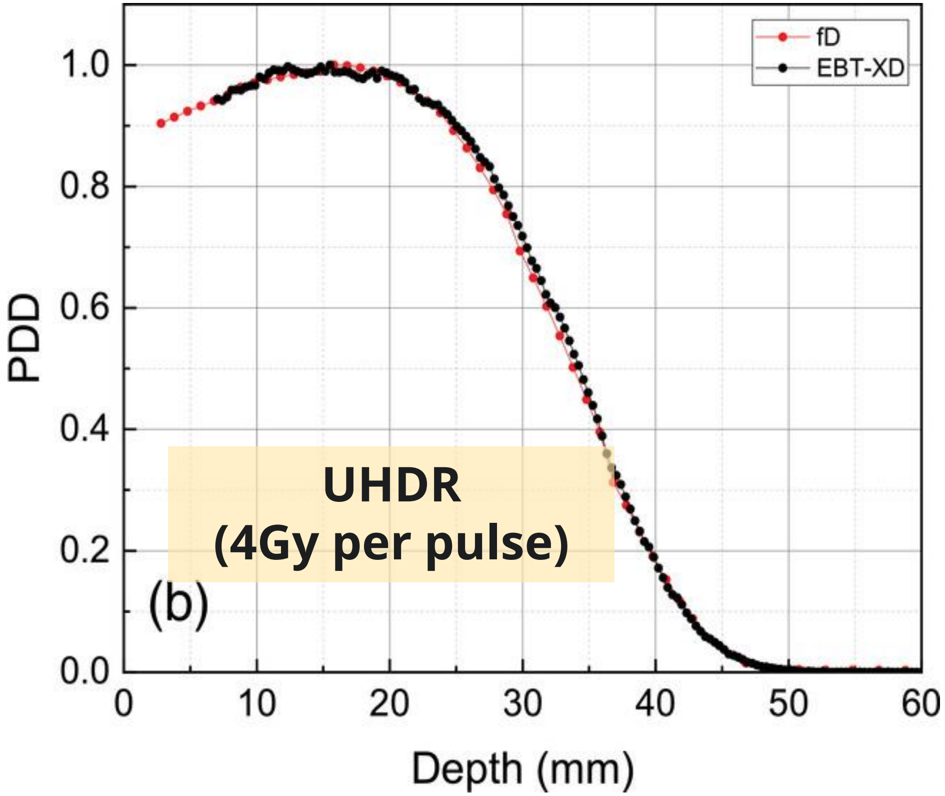

Verona Rinati *et al. Med.Phys.* (2022)

NPL
National Physical Laboratory

Calorimeters

Calorimetry

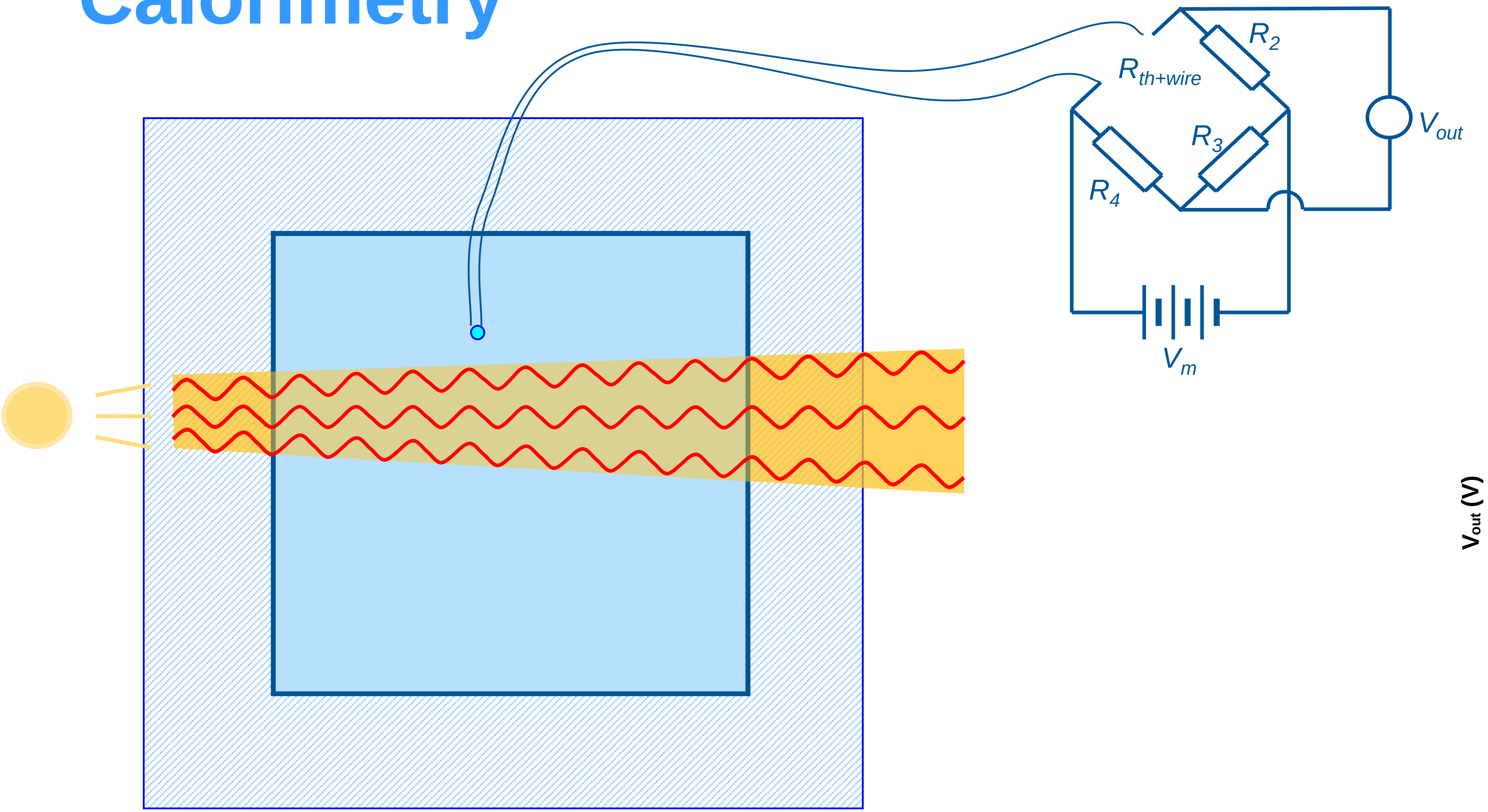

$$D = c \cdot \Delta T$$

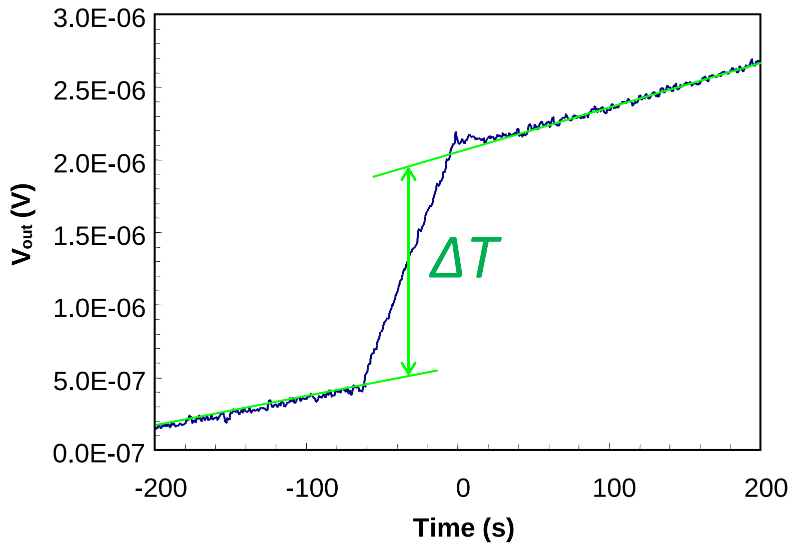

ADVANTAGES

- independent of dose-rate
- linear with dose in UHDR range
- independent of pulse structure
- real-time readout

Calorimetry in UHDR beams

NPL primary standard graphite calorimeter

- Originally developed for use with conventional proton beams, the control and analysis software was reconfigured to enable it to be used with UHDR particle beams
- Consists of graphite discs arranged in a nested construction, maintained under vacuum
- Operated in quasi-adiabatic mode, thermistors detect changes in temperature of the graphite created by energy absorbed from the radiation beam allowing derivation of absorbed dose
- 250 MeV (Varian ProBeam® operating in research mode) at ~65 Gy/s
- The core of the calorimeter was positioned at the isocentre with graphite plates placed in front to position the core at a WET of 5 gcm^{-2}

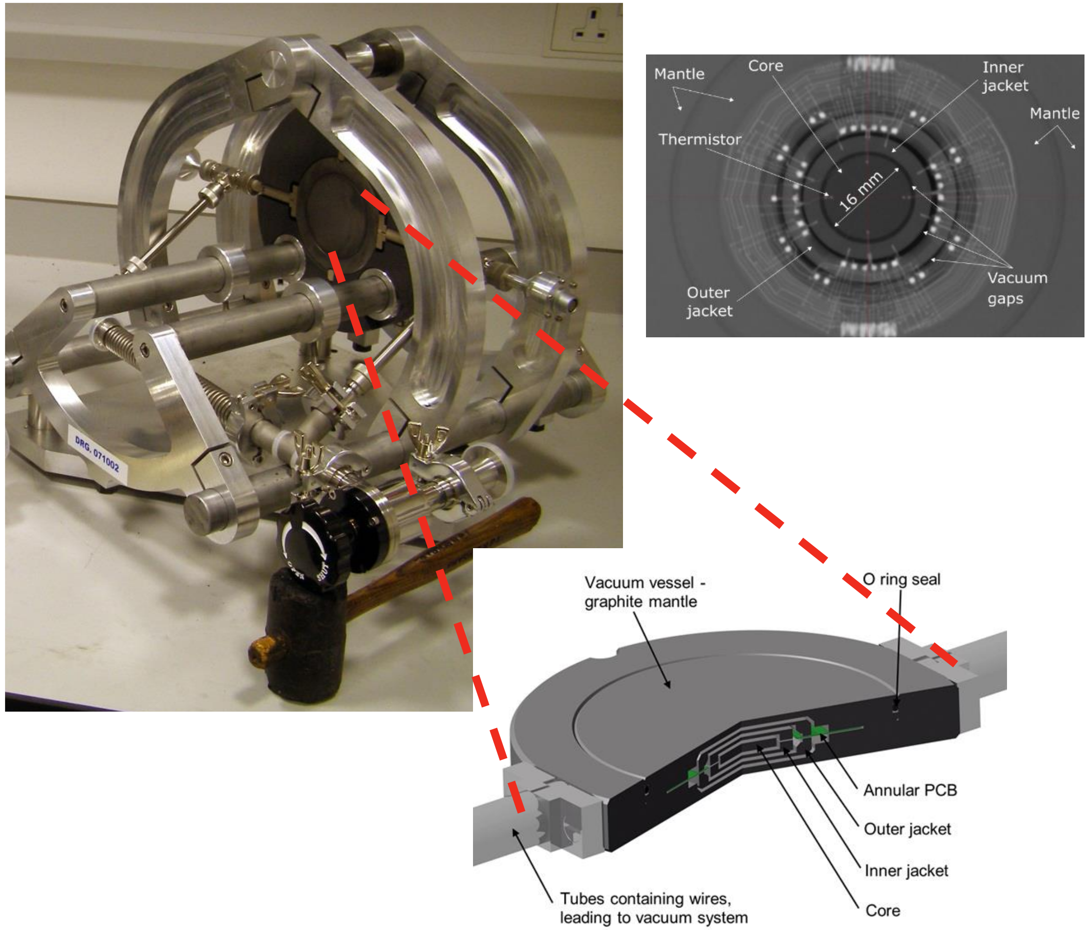

Fig. NPL's primary standard graphite calorimeter.

Calorimetry in UHDR proton beam

National Physical Laboratory

EURAMET

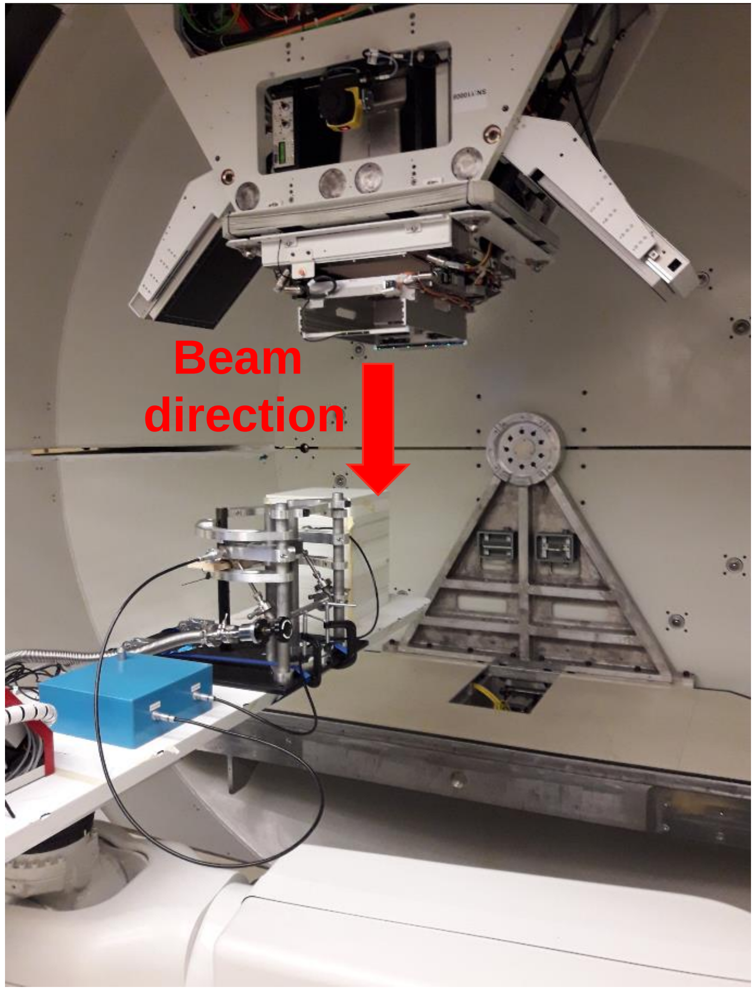

Fig. Experimental setup

Lee, Med.Phys.(2022) accepted

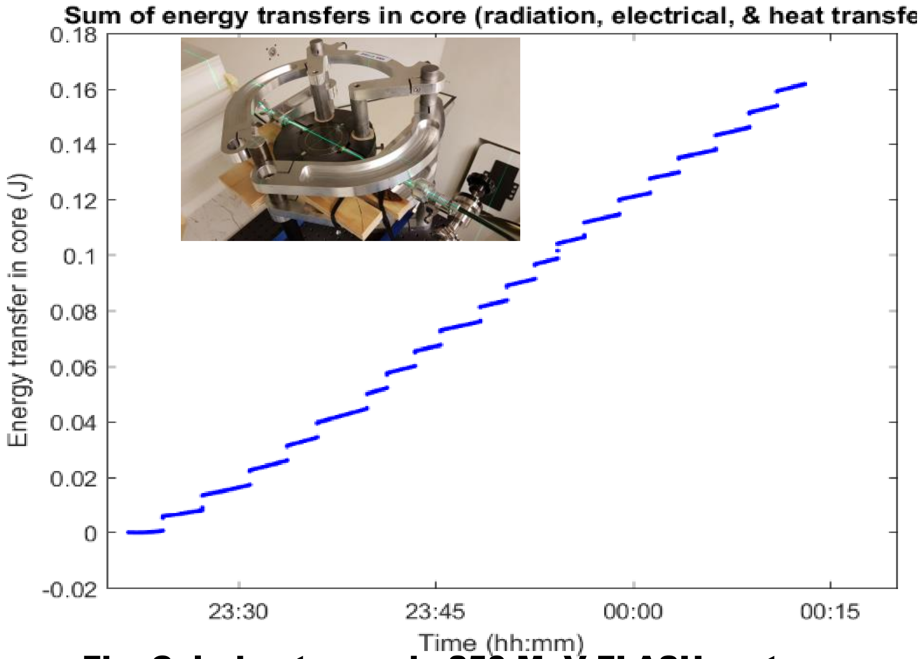

Fig. Calorimetry run in 250 MeV FLASH proton beam

Parameter	Value
c (J·kg^{-1}·K^{-1})	651.57+2.74· (T-273.15)
k_{imp}	1.0016
k_{gap}	1.0029
$s_{w,g}$	1.1210
k_{fl}	0.9713
$k_{z,cal}$	1.0000

Sources of uncertainties (%)	Type A	Type B
Physical dimensions	<0.01	0.09
Electrical calibrations	0.20	0.06
Specific heat capacity	0.08	0.26
k_{imp}, k_{gap}	0.01	0.11
$s_{w,g}$, k_{fl}	0.07	0.71
$k_{z,cal}$	-	0.10
Positioning on beam axis and reference depth	0.06	0.13
PCB	-	0.25
Calorimeter measurements and analysis	0.04	0.15
Total	0.24	0.84
Overall (1σ)	0.9	

Lourenço *et al. Sci.Rep*. under review

	Proton calorimeter				dose to water	
Field size, cm	5 x 6	5 x 8	5 x 10	5 x 12	6 x 5	12 x 5
Mean Dose, Gy	**7.654**	**7.690**	**7.726**	**7.736**	**7.666**	**7.741**
SDOM, %	0.04%	0.04%	0.04%	0.04%	0.04%	0.03%

Small Portable Graphite Calorimeter (SPGC)

NPL National Physical Laboratory

- Originally developed for use with the Clatterbridge ocular proton beam (Palmans et al. 2002). The device was refurbished and integrated with the current control and analysis software developed for UHDR particle beams
- Thermistors are embedded around the circumference of both graphite components
- Operates only in quasi-adiabatic mode
- The core of the calorimeter was positioned at the isocentre with graphite plates placed in front to position the core at a WET of 5 gcm^{-2}

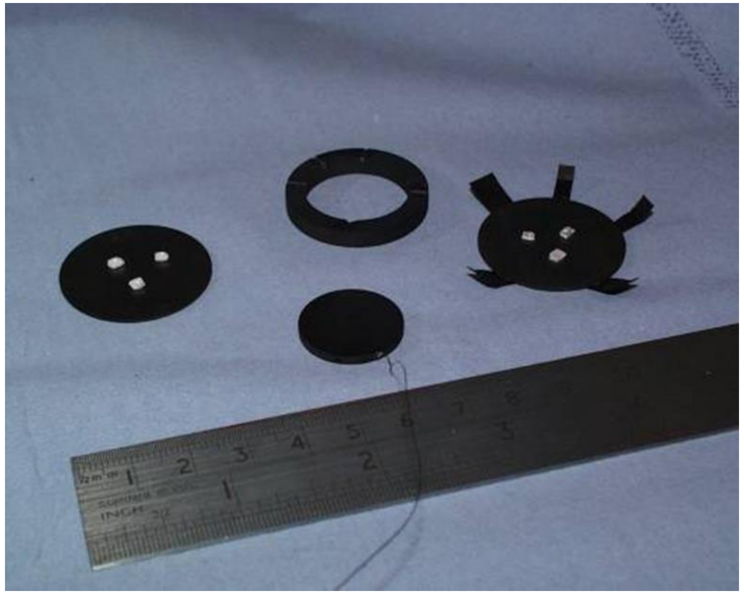

Fig. SPGC

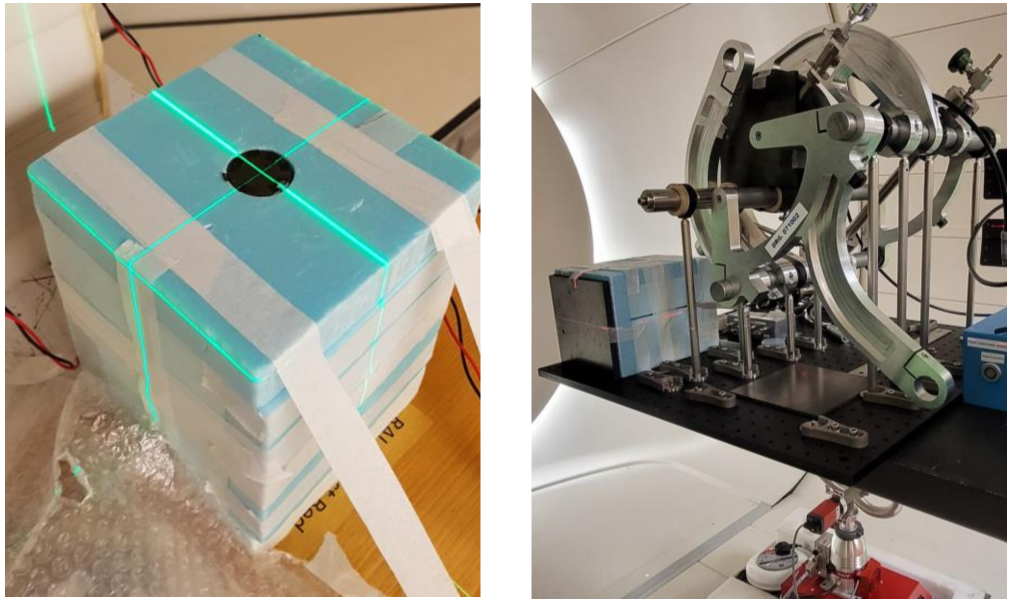

Fig. Experimental setup

	SPGC - provisional dose to water
Field size, cm	5 x 6
Mean Dose, Gy	**7.657**
SDOM, %	0.27%
Type B Uncertainty, %	1.50
Combined Standard Uncertainty, %	1.50
Overall Expanded uncertainty, *k* =1 %	1.50

[UNPUBLISHED - please, do nit distribute]

Al calorimeter

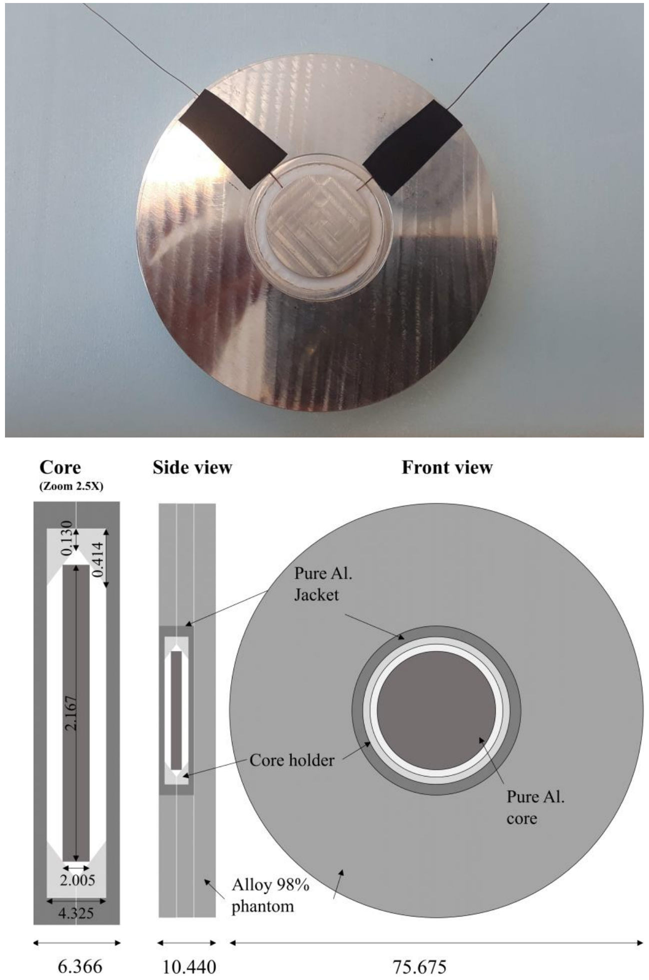

Fig. Construction of Al calorimeter

Courtesy of A. Bourgoin

Linear dose response with varying DPP is equivalent to alanine

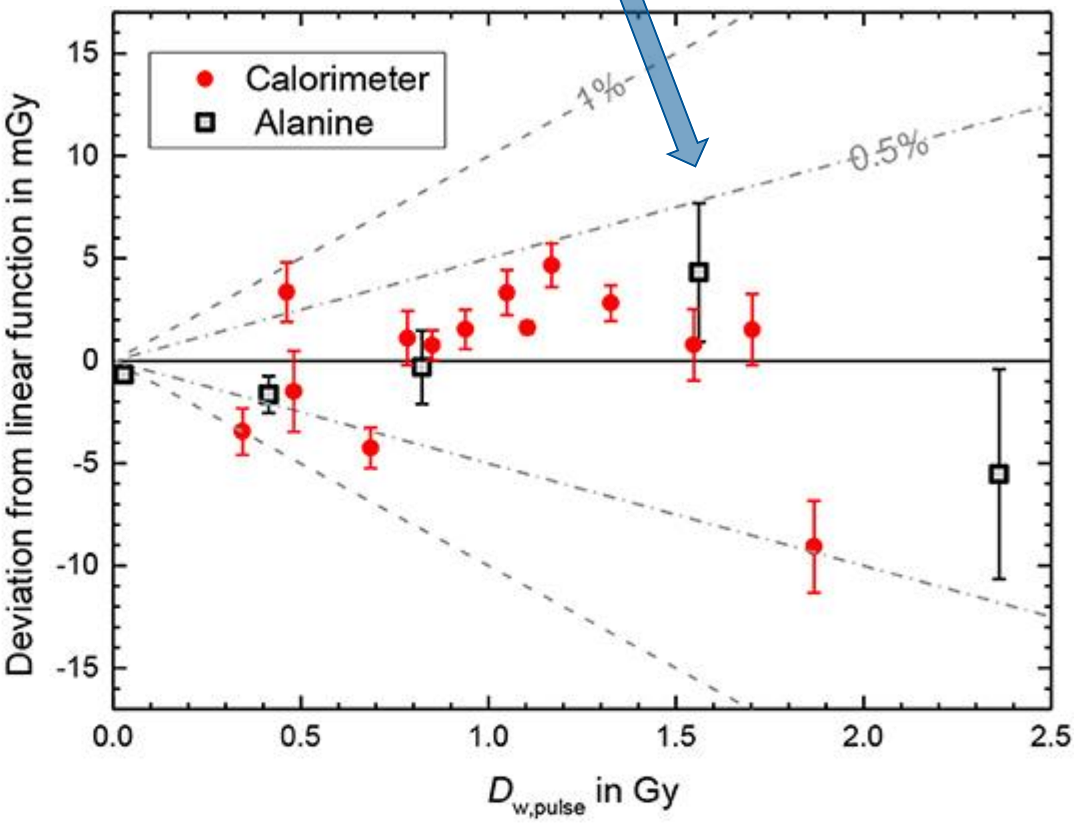

Average deviation was 0.25%

Measured dose deviation from linearity (in mGy) as a function of measured DPP

Bourgoin et al., *Front.in Phys.*, Vol.8, 567340 (2020)

Aerrow – a probe-type graphite calorimeter

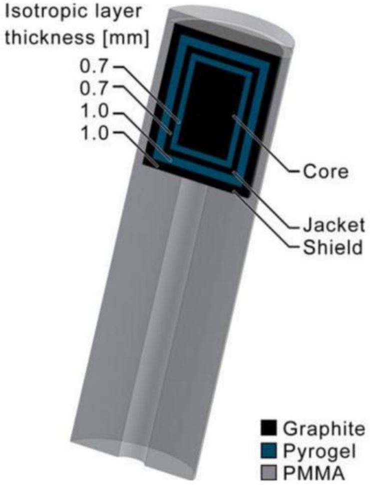

Fig. Aerrow detector

Renaud *et al. Med. Phys*. 45 (1) (2018)

- Developed at McGill
- Made by Sun Nuclear
- Designed for in clinic measurements
- Operating in quasi-adiabatic mode

READING SYSYEM

- Thermistor ready by high stability DMM Agilent

Dose conversion factor

Temp.change

Dose-to-water

$$D_w = c_{gr} \cdot \Delta T \cdot K_{\mathrm{ht}} \cdot \left(\frac{D_{\mathrm{w}}}{D_{\mathrm{gr}}}\right)_{MC}$$

spec.heat capacity

Heat loss corr.

Depth-dose curve

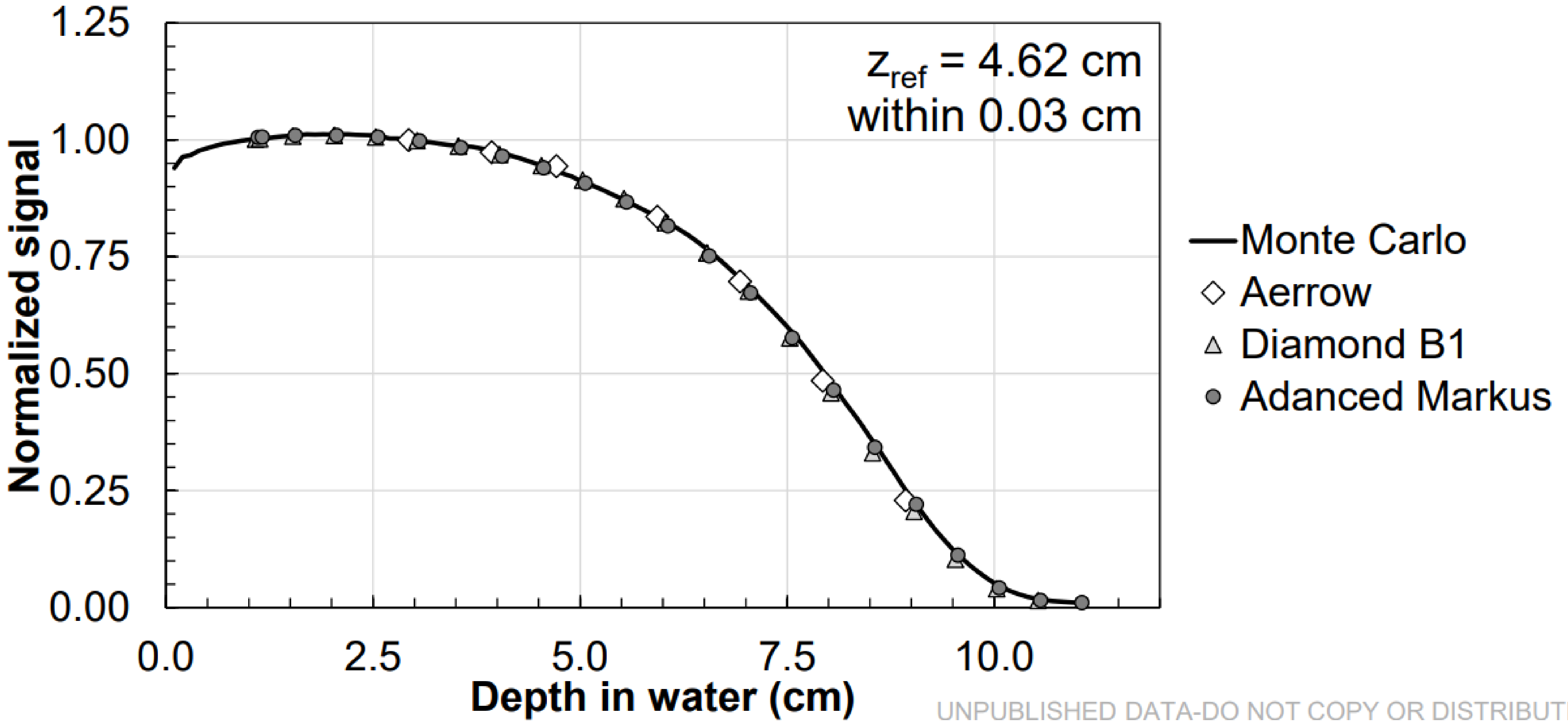

Source: http://uhdpulse-empir.eu/wp-content/uploads/FRPT_Bourgouin_Calorimetry-presentation.pdf

Conclusions

- FLASH RT requires several developments before safe implementation to clinics
- Passive detectors (alanine, film, TLDs) are dose-rate independent, but require post-irradiation processin (not desirable for routine clinical use)
- Commercially available ionization chambers show large deviations at ultra-high dose per pulse (DPP) due to ion recombination.
- Prototypes of parallel plate ionization chambers with very small electrode gap separation are promising candidates for future secondary standard devices for UHDR beams
- Commercially available microDiamond detectors show saturation effects at different DPP levels, however the linear range can be extended to the ultra-high DPP range by reduction of sensitivity and resistance
- Calorimetry-based detectors could become potential dosimetry devices in UHDR beams, but their operation need to be simplified to allow clinical implementation

National Physical Laboratory

The EMPIR initiative is co-funded by the European Union's Horizon 2020 research and innovation programme and the EMPIR Participating States

This project (18HLT04) has received funding from the EMPIR programme co-financed by the Participating States and from the European Union's Horizon 2020 research and innovation programme.

Thank you

anna.subiel@npl.co.uk

http://uhdpulse-empir.eu/